Yan *et al. Thrombosis Journal* (2025) 23:44
https://doi.org/10.1186/s12959-025-00726-8

Thrombosis Journal

RESEARCH Open Access

# Endoplasmic reticulum protein 29 negatively regulates platelet functions and thrombosis in mice

Xiaofeng Yan[1], Yishan Lu[1], Keyu Lv[2], Miao Jiang[1], Chao Fang[2*], Yi Wu[1*] and Aizhen Yang[1*]

## Abstract

**Background** Several members of protein disulfide isomerase (PDI) family with the CXYC active motif such as PDI, ERp57, ERp72, ERp46, ERp5 and TMX1 have important roles in platelet functions and thrombosis. These members contribute to the network of redox regulation of platelet activities. However, whether other PDI family members without the CXYC motif such as ERp29, have a role in these processes remains unknown.

**Aims** To determine the role of ERp29 in platelet functions and thrombosis.

**Methods** The phenotypes of platelet-specific ERp29-deficient (Pf4-Cre/ERp29$^{fl/fl}$) mice were evaluated using tail bleeding assay and laser-induced and $FeCl_3$-induced arterial injury models, as well as venous thrombosis model. In vitro, the functions of ERp29-deficient platelets were assessed in respect to aggregation, adhesion, spreading, clot retraction, granule secretion and integrin αIIbβ3 activation measured by flow cytometry. Redox state of integrin αIIbβ3 thiols was detected using 3-(N-maleimido-propionyl) biotin (MPB) labeling.

**Results** Compared with WT mice, Pf4-Cre/ERp29$^{fl/fl}$ mice exhibited shortened tail-bleeding times, increased platelet accumulation in the two arterial thrombosis models, and enhanced thrombogenesis in the venous thrombosis model. ERp29-deficient platelets had enhanced response in aggregation, ATP release, spreading, clot retraction, αIIbβ3 activation, fibrinogen binding and P-selectin expression. As detected by MPB labeling, the free thiol content of integrin αIIbβ3 in ERp29-deficient platelets were increased compared with WT platelets, suggesting that the role of ERp29 is associated with oxidation of the functional disulfides of integrin αIIb and/or β3 subunits.

**Conclusion(s)** ERp29 is the first disulfide isomerase without the CXYC motif that negatively regulates platelet function. This study provides new insight into the redox network controlling thrombosis.

**Keywords** ERp29, Integrin αIIbβ3, Redox regulation, Platelets, Thrombosis

*Correspondence:
Chao Fang
fangc@hust.edu.cn
Yi Wu
wuy@suda.edu.cn
Aizhen Yang
yangaizhen@suda.edu.cn

[1]Collaborative Innovation Center of Hematology, State Key Laboratory of Radiation Medicine and Prevention, Cyrus Tang Medical Institute, The Fourth Affiliated Hospital of Soochow University, Soochow University, Suzhou, Jiangsu 215123, China
[2]Department of Pharmacology, School of Basic Medicine, Tongji Medical College, State Key Laboratory for Diagnosis and Treatment of Severe Zoonotic Infectious Diseases, Huazhong University of Science and Technology, Wuhan, Hubei 430030, China

## Introduction

Platelets are central mediators of hemostasis and thrombus formation. Upon vascular injury, activated platelets rapidly adhere to damaged endothelial surfaces and exposed subendothelial matrix components through sequential activation processes [1]. Subsequently, activated platelets trigger disulfide bond reduction in integrin αIIbβ3, inducing a conformational shift from low- to high-affinity states. This structural change facilitates fibrinogen binding, thereby promoting platelet aggregation and thrombus formation at injury sites [2, 3]. Although we know that integrin αIIbβ3 activation depends on redox regulation of integrin αIIbβ3 disulfide bonds, which enzymes are responsible for this process has become an important issue [4].

We and other investigators have shown that several members of the protein disulfide isomerase (PDI) family, PDI [5, 6], ERp57 [7, 8], ERp72 [9], ERp46 [10], ERp5 [11–14], TMX4 [15] and TMX1 [16], have been shown to have distinct functions in regulating platelet function and thrombosis via their CXYC active motif. These members contribute to the network of redox regulation of platelet activities. However, whether other PDI family members, especially those without the CXYC motif such as ERp29, have a role in these processes remains unknown.

ERp29, an endoplasmic reticulum (ER)-resident PDI family member, features four structural domains. These include the N-terminal ER localization domain/signal sequence, the b-type PDI domain, the D-domain, and an ER retrieval KEEL (Lys-Glu-Glu-Leu) domain at the C-terminus [17]. Although ERp29 contains a conserved thioredoxin-like PDI domain, it contains only a single cysteine and does not possess any thioredoxin enzymatic activity [18]. Holbrook LM et al. reported that ERp29 is released by platelets and relocates to the cell surface following platelet activation [19]. This study indicates that ERp29 may be involved in the regulation of platelet function. However, its function in platelets needs to be characterized using gene-modified mouse models.

In this study, we found that ERp29 was expressed in platelets and endothelial cells. Using ERp29-knockout mouse models, we found that ERp29 deficiency enhanced platelet aggregation, integrin αIIbβ3 activation, fibrinogen binding, spreading and clot retraction, as well as platelet thrombus formation in vivo. Moreover, we found that the free thiol content of integrin αIIbβ3 in activated ERp29-deficient platelets were increased compared with WT platelets. Thus, ERp29 is the first disulfide isomerase without the CXYC motif that inhibits platelet function and thrombosis.

## Materials and methods

### Materials

Suppliers for antibodies were as follows: anti-mouse integrin αIIbβ3, GPIbα, and GPVI antibodies, PE-labeled JON/A antibodies and Dylight-488-conjugated anti-CD42c from Emfret; PE-conjugated anti-P-selectin antibody from eBioscience; Alexa 647 (Invitrogen)-conjugated anti-human fibrin antibody (59D8) from Antibody System SAS; Rat monoclonal CD41 antibody (MWReg30) from BD Biosciences; Mouse monoclonal anti-αIIb antibody (B-9) and anti-β3 antibody (D-11) from Santa Cruz; Polyclonal anti-vWF antibody from Dako; Polyclonal anti-ERp29 antibody from Abcam; Polyclonal anti-PDI, ERp57 and Transferrin antibody from Abclone; Polyclonal anti-ERp5, ERp46 and GAPDH antibody from Proteintech; Monoclonal anti-ERp72 antibody from HuaBio; IRDye 680-conjugated goat anti-mouse and IRDye 800-conjugated goat anti-rabbit antibodies from LI-COR Bioscience. Additional materials used were: ATP standard and CHRONO-LUME, α-thrombin and collagen from CHRONO-LOG; Convulxin and U46619 from Enzo; Arachidonic acid, A23187 and epinephrine from MCE; 3-( N-maleimido-propionyl) biocytin (MPB) from Molecular Probes; Purified fibrinogen protein from Sigma; Flow chamber plates from Fluxion; PVDF membrane from Millipore.

### Flow cytometry and aggregation and secretion studies of mouse platelets

Flow cytometry studies on mouse platelets were performed using platelet-rich-plasma (PRP) prepared and diluted into Tyrode's buffer as described. The PRP was prepared from blood obtained into acid-citrate dextrose solution through the abdominal aorta [5]. Aggregation studies were performed using washed platelets prepared as described [20]. Platelet concentration was measured using a Sysmex Coulter Counter, and counts were adjusted to $2 \times 10^8$/mL for aggregation studies. Secretion of ATP was monitored in the Chronolog lumi-aggregometer as previously described [21].

### Clot retraction

Clot retraction was performed using washed mouse platelets ($3 \times 10^8$/mL) in Tyrode buffer (pH 7.4) as previously described [22]. Adding fibrinogen (0.5 mg/mL) to washed platelets. Clot retraction was initiated with thrombin (0.3 U/mL), and images were taken at increasing times. Two-dimensional clot size was measured using Image J software, and the percentage of clot size relative to initial suspension volume was determined.

### Platelet spreading on fibrinogen

Platelet spreading on fibrinogen was performed as previously described with minor modifications [23]. Micro

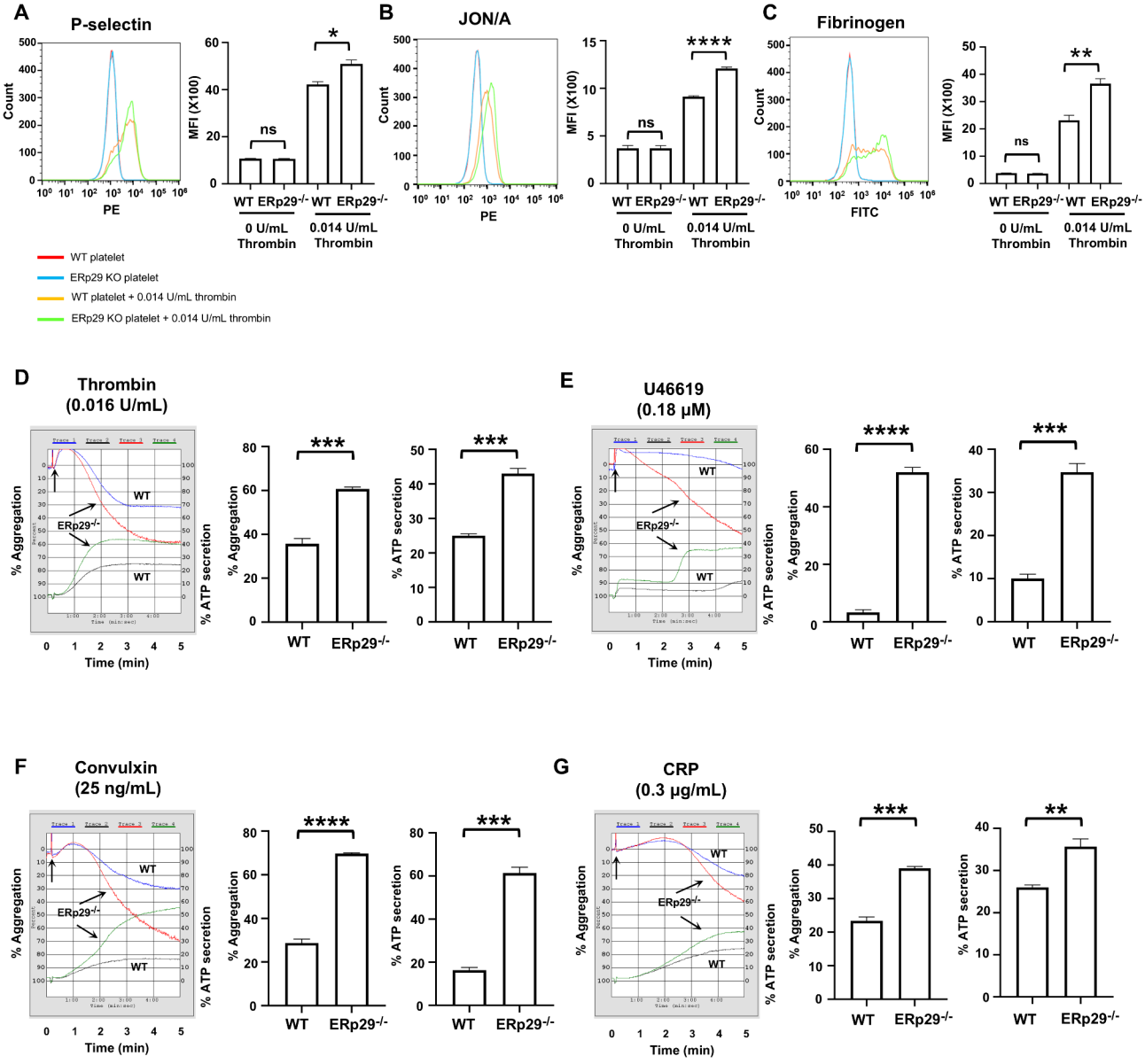


**Fig. 1** ERp29 deficiency potentiates platelet function. (**A**-**C**) ERp29-deficient platelets have enhanced thrombin-induced P-selectin expression (**A**), activation of αIIbβ3 (detected by the JON/A activation-dependent antibody) (**B**) and Fibrinogen binding (**C**). Representative line graphs (left panels) and combined results (right panels); Data are presented as mean ± standard error of the mean (SEM), $n = 3$ for each group, *$P < .05$, **$P < .01$, ****$P < .0001$, Student's t test. ns, not significant. (D-G) Representative aggregation and ATP release tracings (left panels) and combined results (right) showing the enhanced aggregation and ATP release in ERp29-deficient platelets using (**D**) thrombin, (**E**) U46619, (**F**) Convulxin and (**G**) CRP; Mean ± SEM, $n = 3$ for each group, **$P < .01$, ***$P < .001$, ****$P < .0001$, Student's t test. Aggregation and ATP secretion were monitored in the lumi-aggregometer

coverglass-12 mm Dia were coated with 10 μg/mL fibrinogen in 0.1 M NaHCO3 (pH 8.3) in 24 well plates at 4 °C overnight and blocked with 1% bovine serum albumin (BSA) in PBS. Washed platelets ($3 \times 10^7$/mL) in Tyrode buffer were added into wells (200 μL/well) and allowed to spread for 60 min at 37 °C. After unbound platelets were removed by washing, wells were incubated with 4% paraformaldehyde for 30 min at room temperature. F-actin in the adhering platelets was stained by 0.1 μg/mL TRITC-conjugated phalloidin containing 0.1% Triton X-100 for 2 h. Images were collected with a Olympus microscope (confocal), and the average surface area of individual platelets (pixel number) in 15 random fields was quantified using Image J software.

### Bleeding time analysis

Bleeding time assay was performed using a razor blade to transect the mouse-tail 4 mm from the tip, with the tail immersed in a 15-ml test tube containing phosphate-buffered-saline (PBS) at 37 °C [7]. Bleeding times were

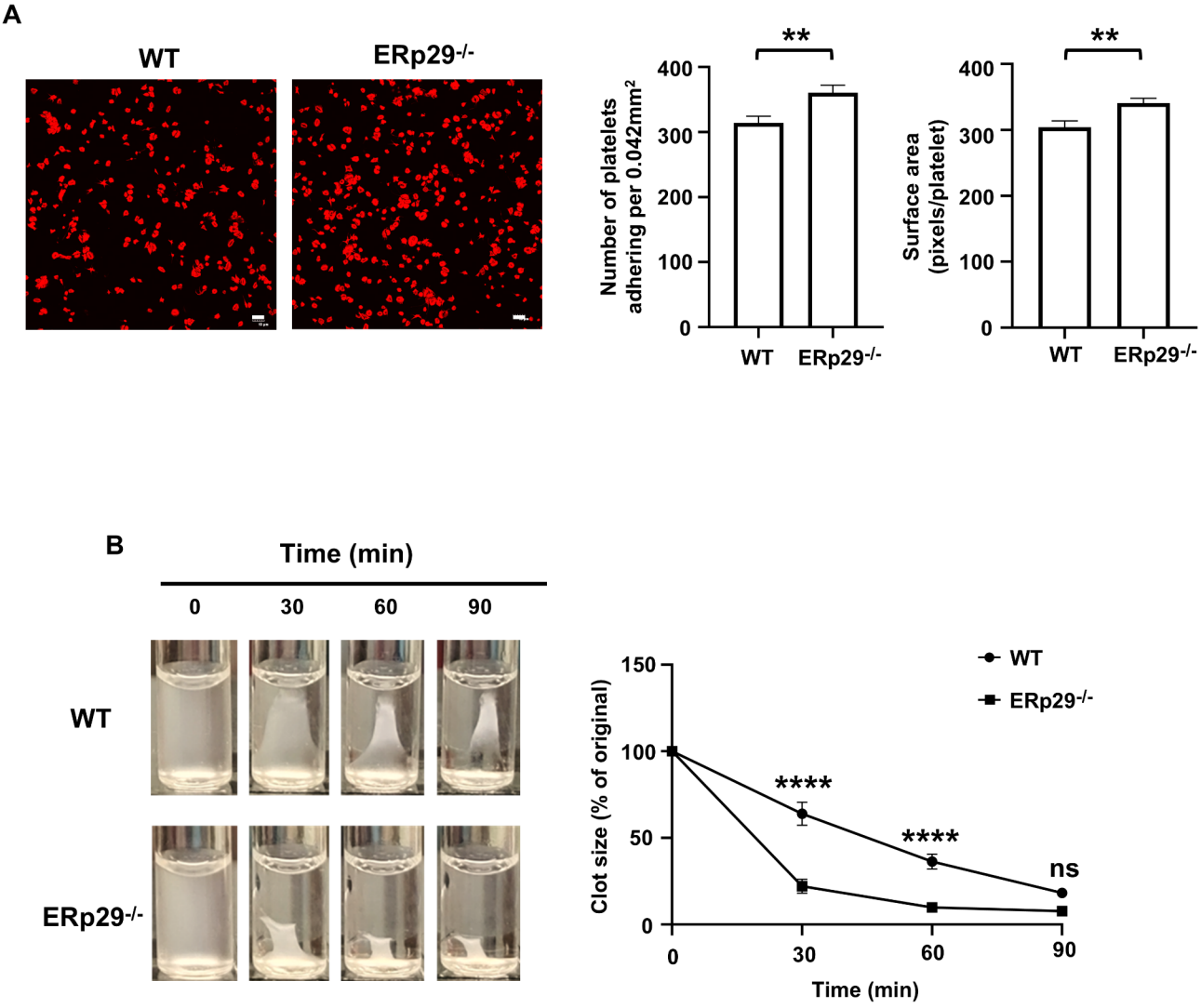


**Fig. 2** ERp29 deficiency enhances platelet spreading and clot retraction. (**A**) Platelet spreading on fibrinogen was induced with thrombin (0.016 U/mL), and adherent platelets were stained with TRITC labeled phalloidin. Representative images are shown, Scale bar, 10 μm. The number and average spreading area of adherent platelets (right) were quantified using Image J in 15 random fields showing the enhancement of platelet spreading in ERp29-deficient platelets; Mean ± SEM, $n = 15$, $^{**}P < .01$, Student's t test. (**B**) Clot retraction was initiated with thrombin (0.3 U/mL), images (left panels) were taken at the indicated times and combined results (right) showing the acceleration of clot retraction in ERp29-deficient platelets. Two-dimensional clot size was measured using Image J and normalized to the clot size at time 0 (clot volume %), Mean ± SEM, $n = 4$, $^{****}P < .0001$, Student's t test. ns, not significant

determined when the bleeding stopped for more than ten seconds. If the bleeding time was longer than 15 min, the assay was stopped and bleeding time was counted as 15 min. The control and experimental groups were matched for age, sex and body weight. The experiments were performed in a single-blinded manner.

#### $FeCl_3$-induced platelet accumulation and thrombosis of the mesenteric artery

To monitor platelet accumulation in vivo, Dylight-488-conjugated anti-CD42c antibody was injected into mice through tail vein, as previously described [16]. Briefly, the mesentery was exteriorized through a midline abdominal incision. A single arteriole was visualized using an OLYMPUS MVX10 fluorescent microscope and its diameter was measured. Vessel injury was generated by placing a 1 × 2 mm patch of No.1 Whatman filter paper soaked in 4% $FeCl_3$ above the exposed artery for 1 min. The filter paper was removed and platelet accumulation observed and photographed every minute for 15 min. The fluorescent intensity (FI) of the platelet accumulation and thrombus formation was analyzed by Image J software. The FI divided by the area analyzed gave the relative FI for each injury and is indicated by FI/μm$^2$. The area analyzed was obtained from the length analyzed multiplied by the diameter of each injured vessel. The length of the thrombi ranged from the beginning of the upstream edge of the thrombi to 1 mm downstream of

this site. Background fluorescent intensity of the uninjured vessels was negligible.

**In vitro thrombosis under flow conditions**

Mouse blood was labeled with Dylight-488-conjugated anti-CD42c antibody and perfused through Bioflux

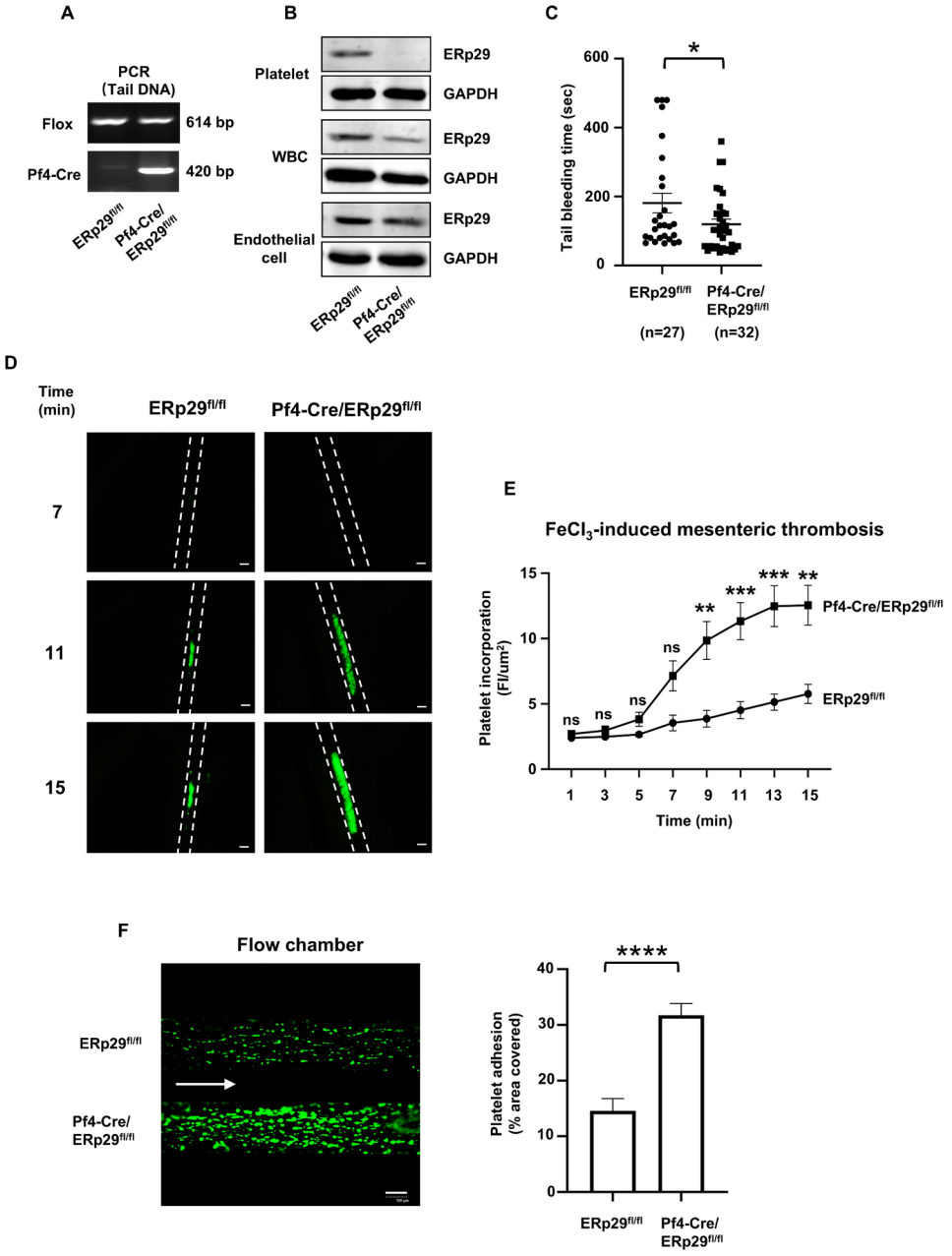


**Fig. 3** ERp29 deficiency shortens the bleeding time and potentiates thrombosis. (**A**-**B**) Characterization of Pf4-Cre/ERp29$^{fl/fl}$ mice. (**A**) PCR products of tail DNA from ERp29$^{fl/fl}$ and Pf4-Cre/ERp29$^{fl/fl}$ mice. The ERp29-floxed allele yielded a 614 bp product and Pf4-Cre recombinase was 420 bp. (**B**) Western blot analysis of ERp29 expression in platelets, white blood cells (WBCs) and endothelial cells (ECs) from ERp29$^{fl/fl}$ and Pf4-Cre/ERp29$^{fl/fl}$ mice. GAPDH serves as loading control. (**C**) Tail bleeding time in ERp29$^{fl/fl}$ and Pf4-Cre/ERp29$^{fl/fl}$ mice; Mean ± SEM. *$P$ < .05, Student's t test. (**D**-**E**) Incorporation of platelets into a growing thrombus in ERp29$^{fl/fl}$ and Pf4-Cre/ERp29$^{fl/fl}$ mice was detected by Dylight-488-conjugated anti-CD42c after $FeCl_3$ (4%)–induced mesenteric arterial injury. Images at 7, 11, and 15 min. The dotted lines mark the vessel wall. Scale bar, 200 µm. The mean artery diameter was 168.1 ± 6.316 µm in ERp29$^{fl/fl}$ mice and 175.8 ± 6.959 µm in Pf4-Cre/ERp29$^{fl/fl}$ mice. (P = not significant, NS). (**E**) Composite of fluorescence intensity (FI) per area analyzed (FI/µm$^2$) in ERp29$^{fl/fl}$ (32 thrombi from 5 mice), Pf4-Cre/ERp29$^{fl/fl}$ (26 thrombi from 4 mice); Mean ± SEM, **$P$ < .01, ***$P$ < .001, ANOVA. ns, not significant. (**F**) Platelet adhesion on collagen under flow conditions. Whole blood was labeled with Dylight-488-conjugated anti-CD42c and perfused through collagen–coated BioFlux plates at 40 dynes/cm$^2$ for 5 min. Scale bar, 100 µm. Platelet adhesion (covered area) was quantified using Image J; Mean ± SEM, ****$P$ < .0001, Student's t test

plates which were pre-coated with collagen (100 μg/mL) for 5 min in a microfluidic whole-blood perfusion assay (Bioflux-200 system) under a shear force of 40 dynes/cm$^2$. Thrombus formation was dynamically monitored via inverted fluorescence microscopy (Olympus IX53). The platelet-covered area was quantified using Image J software [24].

#### Intravital microscopy of laser-induced thrombosis of the cremaster arterioles

Intravital microscopy of the laser-induced injury model of thrombosis was performed as previously described [25, 26]. This experiment examines the cremaster vasculature and thus utilizes only male mice (8 ~ 16 weeks old). Platelets and fibrin were visualized using Dylight-488-conjugated anti-CD42c antibody (0.1 μg/g body weight) and Alexa-647-conjugated anti-fibrin (59D8) antibody (Antibody System, 0.3 μg/g body weight), respectively. Images were analyzed using Slidebook v6.0 (Intelligent Imaging Innovations). The median fluorescence intensity over time was calculated and the area under the curve (AUC) for each thrombus was quantified.

#### Inferior vena cava (IVC) stenosis model

The surgical procedure was performed as described previously [27]. Briefly, the abdomen was opened through a ventral midline laparotomy. The small intestine was gently removed aside and draped with sterile saline-soaked gauze. The IVC was exposed gently and a metal spacer made from 30-gauge needle was placed on the outside of vessel. The IVC and spacer were ligated using a 6.0 nylon suture just below the left renal vein. The spacer was then removed to allow blood flow through the IVC. 48 h after surgery, mice were sacrificed. The weight and length of thrombi from IVC were measured.

#### Labeling of platelet αIIbβ3 with MPB

Washed mouse platelets ($2 \times 10^8$/ml) in BSA-free Tyrode's buffer were incubated with 5 mM EDTA at 37 °C for 1 h. In some experiments, platelets were stimulated with thrombin (0.016 U/mL) for 5 min. For sulfhydryl labeling and quantitation, the membrane impermeant reagent MPB (100 μM) was added, and thiols were labeled, as described previously [9, 28]. Briefly, after a 20 min incubation at room temperature, unreacted MPB was quenched with GSH (200 μM) for 10 min at room temperature. The unreacted GSH was quenched with iodoacetamide (400 μM) for 10 min at room temperature as described. After platelets were washed three times with 1 ml TBS buffer containing 2 mM EDTA, platelet pellet was solubilized with 200 μl lysis buffer (TBS containing protease inhibitor cocktail, 2 mM Na3VO4, 20 μM leupeptin, 1 mM PMSF, and 1% Triton X-100, pH 7.4) and incubated on ice for 30 min. After centrifugation, the supernatant was collected and the protein concentration determined. Platelet lysates were incubated with anti-αIIb antibody (MWReg 30) and protein G beads to immunoprecipitate αIIbβ3. After washing four times with lysis buffer, the relative amount of MPB label per protein on blotting was determined as previously described by using the IRDye® 800CW (Green) Streptavidin (LI-COR) to detect the MPB and IRDye® 680RD (red) goat anti-mouse secondary antibody (LI-COR) to detect the primary mouse anti-αIIb antibody (B-9) and anti-β3 antibody (D-11). The intensity of each band was calculated using Image J program and the ratio of MPB to αIIbβ3 protein.

#### Statistics

Data were analyzed using the statistical software GraphPad Prism 8. For parametric comparison, the values were expressed as the Mean ± SEM, one-way ANOVA (analysis of variance) followed by the Tukey's test was used for multiple groups and the two-tailed Student's t-test was used for 2 groups. For nonparametric comparisons of the area under the curve (AUC) of the laser injury experiments, the Mann Whitney test was used. A P value less than 0.05 was considered significant.

## Results

#### ERp29 is expressed in human platelets and endothelial cells

The expression of ERp29 was detected by immunoblotting and found that human platelets and endothelial cells (HUVECs) expressed ERp29 protein (supplemental Fig. 1A). Moreover, we found that human platelets expressed 18,900 ERp29 molecules per platelet (supplemental Fig. 1B), which is similar to the level of PDI molecules (32,000 per platelet) reported previously [6].

#### Generation and characterization of ERp29-knockout mice

To determine the role of ERp29 in thrombosis, first, ERp29-knockout mice were generated, using the knockout-first conditional-ready strategy [29] (supplemental Fig. 2A). Littermate wild-type (WT) and ERp29-knockout (ERp29$^{-/-}$, knockout first) mice were confirmed by PCR analysis (supplemental Fig. 2B). To test the knockout efficiency of ERp29$^{-/-}$ mice, the protein levels of ERp29 were measured using western blotting, showing that platelets, white blood cells, endothelial cells, heart, liver, spleen, lung and kidney from ERp29-knockout mice did not express ERp29 protein (supplemental Fig. 2C), indicating the successful global knockout of ERp29. Platelet counts and volume were comparable to those of wild-type control mice (supplemental Fig. 3A-B). Platelets from ERp29$^{-/-}$ mice presented normal expression of the major platelet surface glycoproteins (GPIbα, GPVI and αIIbβ3) (supplemental Fig. 3C-E). The size

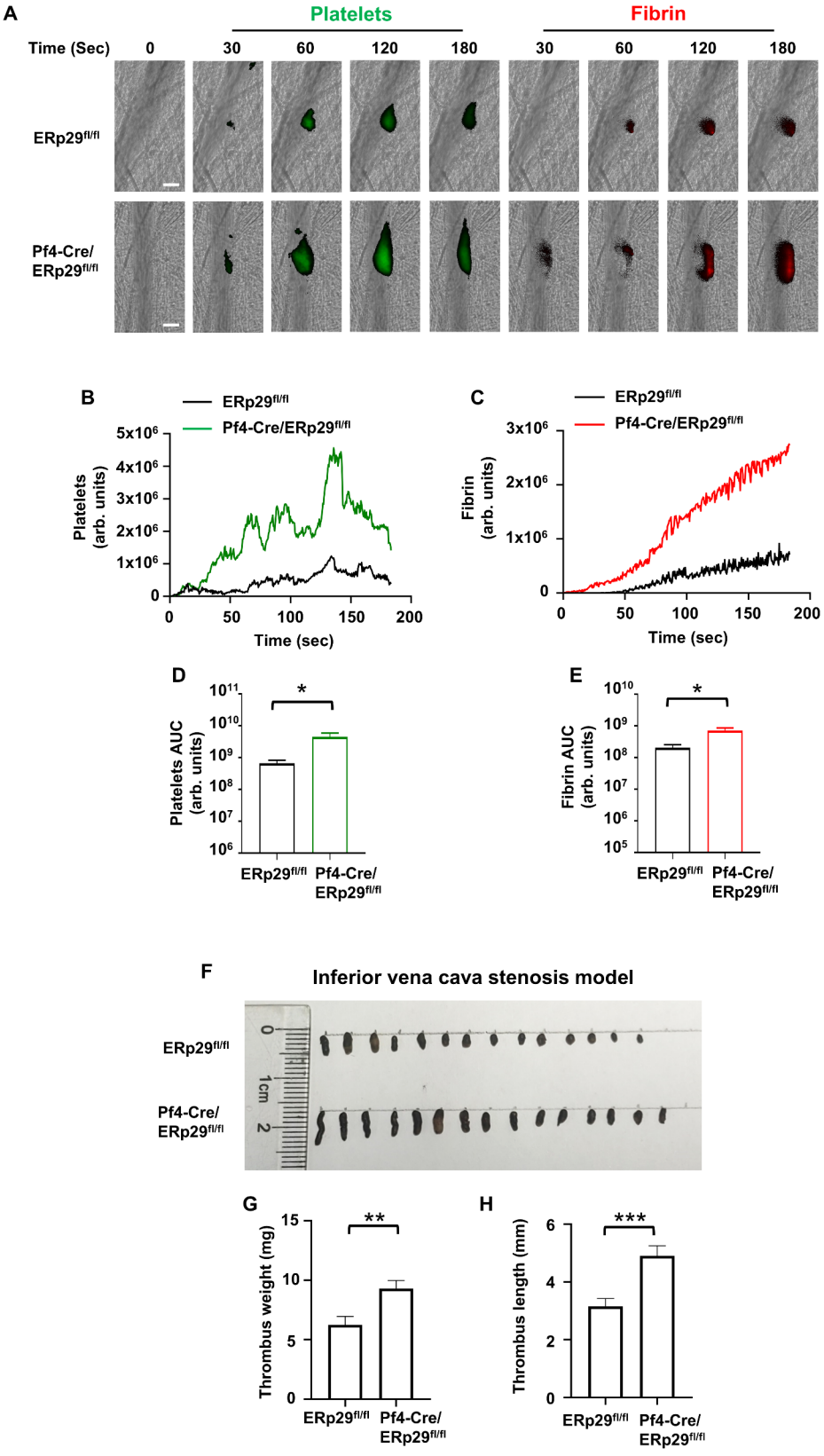


**Fig. 4** (See legend on next page.)

(See figure on previous page.)

**Fig. 4** ERp29 deficiency potentiates platelet accumulation and fibrin deposition and venous thrombosis. (**A**) Representative images of platelet accumulation (Green) and fibrin generation (Red), as visualized by Dylight-488-conjugated anti-CD42c and Alexa-647-conjugated fibrin (59D8) antibody, respectively, at indicated time points following laser injury in the cremaster arterioles in ERp29$^{fl/fl}$ and Pf4-Cre/ERp29$^{fl/fl}$ mice. Scale bar, 30 μm. The median fluorescence intensity of platelets (**B**) and fibrin (**C**) were calculated and plotted over time. The area under the curve (AUC) for platelets (**D**) and fibrin (**E**) were analyzed from each individual thrombus in the two groups. Data are presented as Mean ± SEM and analyzed by two-tailed Mann–Whitney U-test, **P* < .05. The data were obtained from 26 thrombi in 3 mice for each experimental condition. (**F**-**H**) Pf4-Cre/ERp29$^{fl/fl}$ mice ($n = 15$) and control littermate ERp29$^{fl/fl}$ mice ($n = 14$) were subjected to IVC stenosis for 48 h. Thrombi were extracted 48 h after surgery. (**F**) Representative image showing the different size of thrombi from ERp29$^{fl/fl}$ and Pf4-Cre/ERp29$^{fl/fl}$ mice after 48 h of stenosis. (**G**) Thrombus weight and (**H**) length at 48 h were quantified respectively. Mean ± SEM, ***P* < .01; ****P* < .001, Student's t test

and morphology of platelets and number of granule were comparable between ERp29$^{-/-}$ and littermate control wild-type mice, as determined by using transmission electron microscopy (supplemental Fig. 3F).

### Coagulation function and vWF biosynthesis in ERp29-knockout mice are normal

Activated partial thromboplastin time (aPTT), prothrombin time (PT) and thrombin time (TT) in plasma from ERp29$^{-/-}$ mice were normal (supplemental Fig. 4A-C), suggesting that these mice have not coagulopathy. Since von Willebrand factor (vWF) plays an important role in thrombosis, its levels in plasma and epinephrine-induced vWF release in ERp29$^{-/-}$ mice were measured using western blotting, transferrin serves as loading control, showing that vWF levels in plasma were comparable to those of wild-type control mice and epinephrine-induced vWF release was normal (supplemental Fig. 4D, E). In addition, vWF multimer was normal in ERp29$^{-/-}$ mice as analyzed by SDS-agarose gel electrophoresis (supplemental Fig. 4F).

### ERp29 deficiency potentiates platelet functions

Thrombin-induced P-selectin surface expression, αIIbβ3 activation and fibrinogen binding were consistently elevated in ERp29-deficient platelets (Fig. 1A-C). Compared with the wild-type platelets, ERp29-deficient platelets exhibited significantly increased in aggregation and ATP release in response to thrombin, convulxin, collagen-related peptide (CRP) and thromboxane A2 analog, U46619 (Fig. 1D-G). Calcium ionophore, A23187 and arachidonic acid (AA)-induced aggregation were also enhanced (supplemental Fig. 5A, B). These results suggested that ERp29 inhibits platelet functions.

### ERp29 deficiency enhances platelet spreading and clot retraction

Platelet spreading and clot retraction are processes in which the cytoskeleton of platelets reorganizes driven by integrin αIIbβ3-mediated outside-in signaling, and are important for hemostasis and thrombosis in response to vascular injury. To determine whether ERp29 plays a role in platelet spreading and clot retraction, we analyzed adhesion and spreading of ERp29-deficient and wild-type platelets, and found that ERp29 deficiency enhanced fibrinogen-mediated platelet adhesion and spreading (Fig. 2A). In accordance with this finding, clot retraction was also significantly enhanced in ERp29-deficient platelets (Fig. 2B). These results suggested that ERp29 is also involved in integrin αIIbβ3-mediated outside-in signaling.

### ERp29 deficiency shortens bleeding time and potentiates thrombosis

To further determine the specific role of platelet ERp29 in platelet function and thrombosis, platelet-specific ERp29-knockout (Pf4-Cre/ERp29$^{fl/fl}$) mice were generated (supplemental Fig. 2D). Genotyping of Pf4-Cre/ERp29$^{fl/fl}$ mice showed the homozygous floxed allele and the presence of the Cre gene (Fig. 3A). Pf4-Cre/ERp29$^{fl/fl}$ mice did not express ERp29 protein in platelets, but express ERp29 protein in white blood cells and endothelial cells (Fig. 3B). In addition, the expression of ERp29 was also detected in the heart, liver, spleen, lung and kidney in Pf4-Cre/ERp29$^{fl/fl}$ mice (supplemental Fig. 2E). The levels of PDI, ERp57, ERp72, ERp5 and ERp46 in ERp29-deficient platelets were comparable with wild-type platelets (supplemental Fig. 6A), indicating successful targeting of ERp29. Using Pf4-Cre/ERp29$^{fl/fl}$ mice, we observed that platelet ERp29 deficiency shortened mouse tail bleeding times (Fig. 3C). In the $FeCl_3$-induced mesenteric artery injury model, the incorporation of platelets into the thrombus of Pf4-Cre/ERp29$^{fl/fl}$ mice was also substantially increased compared with that of control ERp29$^{fl/fl}$ mice (Fig. 3D-E). Furthermore, under arterial flow conditions, ERp29 deficiency significantly promoted thrombus formation in vitro (Fig. 3F). From these data, it is indicated that platelet ERp29 inhibits hemostasis and arterial thrombosis.

### ERp29 deficiency potentiates platelet accumulation, fibrin deposition and venous thrombosis

To confirm the role of ERp29 in platelet accumulation in a second injury model and to analyze fibrin deposition at the same time, we used a laser-induced cremaster arteriole injury model, and Pf4-Cre/ERp29$^{fl/fl}$ mice exhibited a significant increase in platelet accumulation and fibrin deposition (Fig. 4A-E). In addition, we investigated the role of ERp29 in venous thrombus formation using a mouse inferior vena cava (IVC) stenosis

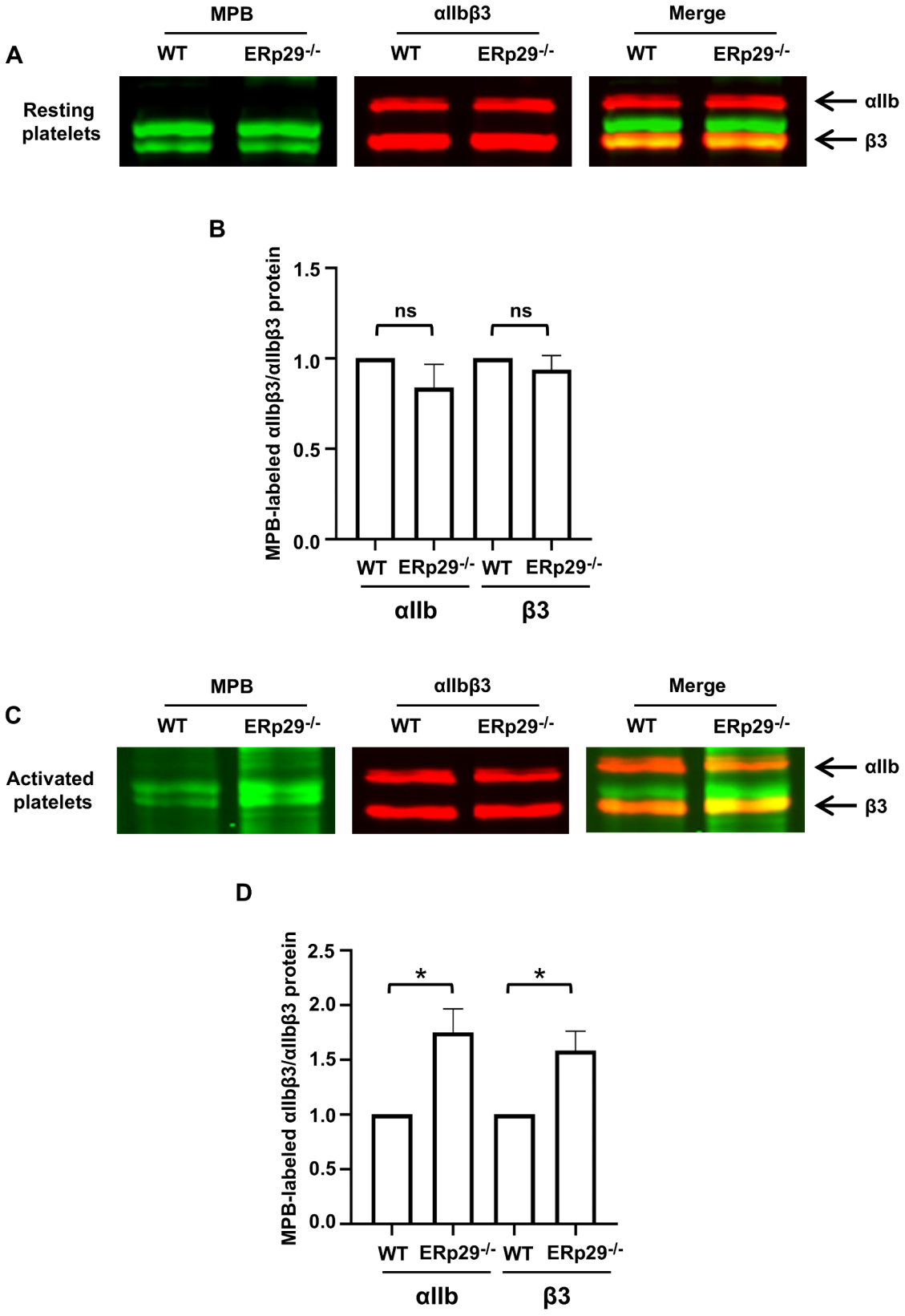


**Fig. 5** (See legend on next page.)

(See figure on previous page.)

**Fig. 5** ERp29 deficiency increases thiols of the αIIbβ3 integrin in activated platelets. (**A**-**D**) Thiols are increased in αIIbβ3 on the surface of activated ERp29 deficient platelets. Platelets from wild-type and ERp29 knockout mice were activated with thrombin (0.016 U/mL) for 5 min followed by MPB labeling. After platelet lysis, αIIbβ3 was immunoprecipitated. The labeled thiols were detected by blotting with fluorescence conjugated streptavidin. The membranes were re-probed with anti-αIIb and anti-β3 antibodies, and the MPB label was normalized to the protein density. Representative blot (**A**, **C**), cumulative data (**B**, **D**); Mean ± SEM, $n = 3$, $^*P < .05$, Student's t test. ns, not significant

model. Compared with control ERp29$^{fl/fl}$ mice, Pf4-Cre/ERp29$^{fl/fl}$ mice displayed significantly increased weight and length of thrombus (Fig. 4F-H). These results suggested that platelet ERp29 inhibits both arterial and venous thrombosis.

### ERp29 deficiency increases thiols of the αIIbβ3 integrin in activated platelets

The redox regulation of integrin αIIbβ3 disulfides is very important for platelet activation. We and others have previously shown that the PDI family members, including ERp57 [8], ERp72 [9], ERp46 [10] and PDI [5], enhance platelet aggregation by reducing integrin αIIbβ3 disulfides; in contrast, TMX1 [16] inhibits platelet aggregation by oxidizing integrin αIIbβ3 disulfides. It is unknow whether ERp29 affect αIIbβ3 disulfides. MPB labeling revealed increased free thiol content in activated αIIbβ3 integrins from ERp29-deficient platelets relative those from wild-type platelets (Fig. 5C, D); however, it had no difference in resting platelets (Fig. 5A, B). This suggests that the role of ERp29 is associated with oxidation of the functional disulfides of integrin αIIbβ3 subunits in response to platelet activation.

## Discussion

In this study, using a new genetically modified mouse model of ERp29 knockout and platelet-specific ERp29 deficiency, we provide the first evidence that platelet ERp29 inhibits platelet functions, including platelet aggregation, ATP release, spreading, clot retraction, αIIbβ3 activation, fibrinogen binding and P-selectin surface expression. In the platelet aggregation assay, we found that ERp29-deficient platelets both showed enhanced platelet aggregation in response to various stimulants such as thrombin, convulxin, CRP and U46619 (Fig. 1D-G), as well as A23187 and arachidonic acid (supplemental Fig. 5A, B), suggesting that ERp29 is likely to act on a common pathway of platelet activation. We also found that ERp29-deficient platelets enhanced platelet spreading and clot retraction, suggesting that ERp29 is also involved in platelet integrin αIIbβ3-mediated outside-in signaling. These results indicate that ERp29 is likely to regulate the activation of integrin αIIbβ3.

Pf4-Cre/ERp29$^{fl/fl}$ mice lacking platelet ERp29 displayed shortened tail-bleeding times and increased platelet accumulation in the two arterial thrombosis models, as well as fibrin deposition in a laser-induced arterial thrombosis. Additionally, Pf4-Cre/ERp29$^{fl/fl}$ mice exhibited enhanced thrombogenesis in the venous thrombosis model. Although these models differ in injury mechanisms, vessel size, and hemodynamics, the consistent phenotype under these different conditions indicates that platelet-derived ERp29 inhibits both platelet accumulation and fibrin deposition in arterial thrombosis and venous thrombosis in mice, which is not the case for other reported PDI family members. It will be interesting to investigate how platelet-derived ERp29 regulates coagulation and venous thrombosis.

Holbrook LM et al. reported that ERp29 is released by platelets and relocate to the cell surface following platelet activation [19]. However, the amount of ERp29 released by platelets is small. Although ERp29 is a PDI-like protein, it lacks a thioredoxin domain and is therefore likely redox inactive. In this way, ERp29 is unique, and functions as a chaperone or escort of immature client protein, stabilizing clients and facilitating their transport from the ER to the Golgi for maturation [17], such as proinsulin [30], and thyroglobulin [31] in secretory cells and non-secretory membrane proteins including Cx43 hemichannels [32], CFTR [33] and ENaC [34] in epithelial tissue. These findings suggest that ERp29 may participate in quality control processes during membrane protein biogenesis in the endoplasmic reticulum.

The free thiol content of integrin αIIbβ3 is increased in activated platelets [35]. We found that the free thiol content of integrin αIIbβ3 in activated ERp29-deficient platelets was increased than that in wild-type platelets. However, ERp29 does not possess redox activity, and we found no difference in the ratio of GSH to GSSG between wildtype and ERp29-deficient platelets in either resting or activated state (supplemental Fig. 6B). How ERp29 regulates the disulfide bond of αIIbβ3 is an interesting but complex question, this is also a limitation of our study.

Several secreted enzymes of the PDI family with CXYC motif, such as PDI [5], ERp57 [8], ERp72 [9], ER46 [10] and TMX4 [15], have been shown to support platelet activation through reducing the disulfide bond of integrin αIIbβ3, and ERp5 inhibits platelet activation through binding to integrin αIIbβ3 blocking its ligand binding [14] or cleaving β3 disulfide C177-C184 to decrease the ligand binding affinity [36]. and TMX1 [16] has an inhibitory role through oxidizing the disulfide bond of integrin αIIbβ3, demonstrating that the PDI family members can both positively and negatively regulate platelet function. Our current study has revealed that ERp29 is the

first member without CXYC motif of this network and revealed a CXYC motif-independent pathway for remodeling in the disulfide bond of integrin αIIbβ3.

In conclusion, ERp29 is the first disulfide isomerase without the CXYC motif that negatively regulates platelet functions and thrombosis. These findings reveal the complex regulatory mechanism of PDI family enzymes in platelet activation and thrombosis.

## Supplementary Information

The online version contains supplementary material available at https://doi.org/10.1186/s12959-025-00726-8.

Supplementary Material 1

Supplementary Material 2

### Author contributions

X.Y. and Y.W. wrote the main manuscript text; X.Y., A.Y. and Y.W. designed and performed research, collected, analyzed data; K.L. and C.F. assisted with the in vivo thrombosis models and interpretation; Y.L. and M.J. helped with the study design and data analysis; A.Y. and Y.W. supervised the research. All authors reviewed the manuscript.

### Funding

This work was supported by grants from the National Natural Science Foundation of China (82170129, 81970128, 82470132, 81770138, 31970890, 82270136, 82200147), the Translational Research Grant of NCRCH (2020ZKPA02, 2020WSA04), the Jiangsu Provincial Medical Innovation Center (CXZX202201), the collaboration fund from State Key Laboratory of Radiation Medicine and Protection (GZN1201802), the Priority Academic Program Development of Jiangsu Higher Education Institutions (PAPD).

### Data availability

No datasets were generated or analysed during the current study.

## Declarations

### Ethics approval and consent to participate

Not applicable.

### Consent for publication

Not applicable.

### Competing interests

The authors declare no competing interests.

Received: 5 March 2025 / Accepted: 15 April 2025
Published online: 07 May 2025

### References

1. Furie B, Furie BC. Mechanisms of thrombus formation. N Engl J Med. 2008;359:938–49. https://doi.org/10.1056/NEJMra0801082.
2. O'Neill S, Robinson A, Deering A, Ryan M, Fitzgerald DJ, Moran N. The platelet integrin alpha IIbbeta 3 has an endogenous thiol isomerase activity. J Biol Chem. 2000;275:36984–90. https://doi.org/10.1074/jbc.M003279200.
3. Zhu J, Luo BH, Xiao T, Zhang C, Nishida N, Springer TA. Structure of a complete integrin ectodomain in a physiologic resting state and activation and deactivation by applied forces. Mol Cell. 2008;32:849–61. https://doi.org/10.1016/j.molcel.2008.11.018.
4. Shattil SJ, Kim C, Ginsberg MH. The final steps of integrin activation: the end game. Nat Rev Mol Cell Biol. 2010;11:288–300. https://doi.org/10.1038/nrm2871.
5. Zhou J, Wu Y, Wang L, Rauova L, Hayes VM, Poncz M, et al. The C-terminal CGHC motif of protein disulfide isomerase supports thrombosis. J Clin Invest. 2015;125:4391–406. https://doi.org/10.1172/jci80319.
6. Kim K, Hahm E, Li J, Holbrook LM, Sasikumar P, Stanley RG, et al. Platelet protein disulfide isomerase is required for thrombus formation but not for hemostasis in mice. Blood. 2013;122:1052–61. https://doi.org/10.1182/blood-2013-03-492504.
7. Wu Y, Ahmad SS, Zhou J, Wang L, Cully MP, Essex DW. The disulfide isomerase ERp57 mediates platelet aggregation, hemostasis, and thrombosis. Blood. 2012;119:1737–46. https://doi.org/10.1182/blood-2011-06-360685.
8. Wang L, Wu Y, Zhou J, Ahmad SS, Mutus B, Garbi N, et al. Platelet-derived ERp57 mediates platelet incorporation into a growing thrombus by regulation of the AIIbβ3 integrin. Blood. 2013;122:3642–50. https://doi.org/10.1182/blood-2013-06-506691.
9. Zhou J, Wu Y, Chen F, Wang L, Rauova L, Hayes VM, et al. The disulfide isomerase ERp72 supports arterial thrombosis in mice. Blood. 2017;130:817–28. https://doi.org/10.1182/blood-2016-12-755587.
10. Zhou J, Wu Y, Rauova L, Koma G, Wang L, Poncz M, et al. A novel role for Endoplasmic reticulum protein 46 (ERp46) in platelet function and arterial thrombosis in mice. Blood. 2022;139:2050–65. https://doi.org/10.1182/blood.2021012055.
11. Jordan PA, Stevens JM, Hubbard GP, Barrett NE, Sage T, Authi KS, et al. A role for the thiol isomerase protein ERP5 in platelet function. Blood. 2005;105:1500–7. https://doi.org/10.1182/blood-2004-02-0608.
12. Passam FH, Lin L, Gopal S, Stopa JD, Bellido-Martin L, Huang M, et al. Both platelet- and endothelial cell-derived ERp5 support thrombus formation in a laser-induced mouse model of thrombosis. Blood. 2015;125:2276–85. https://doi.org/10.1182/blood-2013-12-547208.
13. Lay AJ, Dupuy A, Hagimola L, Tieng J, Larance M, Zhang Y, et al. Endoplasmic reticulum protein 5 attenuates platelet Endoplasmic reticulum stress and secretion in a mouse model. Blood Adv. 2023;7:1650–65. https://doi.org/10.1182/bloodadvances.2022008457.
14. Sun K, Zhang Y, Yang A, Zhang Y, Zhao Z, Yan X, et al. Extracellular thiol isomerase ERp5 regulates integrin AIIbβ3 activation by Inhibition of fibrinogen binding. Platelets. 2025;36:2455743. https://doi.org/10.1080/09537104.2025.2455743.
15. Zhao Z, Wang Y, Yang A, Lu Y, Yan X, Peng M, et al. A novel role for thioredoxin-related transmembrane protein TMX4 in platelet activation and thrombus formation. J Thromb Haemost. 2025;23:277–92. https://doi.org/10.1016/j.jtha.2024.09.007.
16. Zhao Z, Wu Y, Zhou J, Chen F, Yang A, Essex DW. The transmembrane protein disulfide isomerase TMX1 negatively regulates platelet responses. Blood. 2019;133:246–51. https://doi.org/10.1182/blood-2018-04-844480.
17. Brecker M, Khakhina S, Schubert TJ, Thompson Z, Rubenstein RC. The probable, possible, and novel functions of ERp29. Front Physiol. 2020;11:574339. https://doi.org/10.3389/fphys.2020.574339.
18. Galligan JJ, Petersen DR. The human protein disulfide isomerase gene family. Hum Genomics. 2012;6:6. https://doi.org/10.1186/1479-7364-6-6.
19. Holbrook LM, Watkins NA, Simmonds AD, Jones CI, Ouwehand WH, Gibbins JM. Platelets release novel thiol isomerase enzymes which are recruited to the cell surface following activation. Br J Haematol. 2010;148:627–37. https://doi.org/10.1111/j.1365-2141.2009.07994.x.
20. Wu Y, Suzuki-Inoue K, Satoh K, Asazuma N, Yatomi Y, Berndt MC, et al. Role of Fc receptor gamma-chain in platelet glycoprotein Ib-mediated signaling. Blood. 2001;97:3836–45. https://doi.org/10.1182/blood.v97.12.3836.
21. Essex DW, Li M. Protein disulphide isomerase mediates platelet aggregation and secretion. Br J Haematol. 1999;104:448–54. https://doi.org/10.1046/j.1365-2141.1999.01197.x.
22. Huang Y, Joshi S, Xiang B, Kanaho Y, Li Z, Bouchard BA, et al. Arf6 controls platelet spreading and clot Retraction via integrin AIIbβ3 trafficking. Blood. 2016;127:1459–67. https://doi.org/10.1182/blood-2015-05-648550.
23. Flevaris P, Li Z, Zhang G, Zheng Y, Liu J, Du X. Two distinct roles of mitogen-activated protein kinases in platelets and a novel Rac1-MAPK-dependent integrin outside-in Retractile signaling pathway. Blood. 2009;113:893–901. https://doi.org/10.1182/blood-2008-05-155978.
24. Wang X, Wei G, Ding Y, Gui X, Tong H, Xu X, et al. Protein tyrosine phosphatase PTPN22 negatively modulates platelet function and thrombus formation. Blood. 2022;140:1038–51. https://doi.org/10.1182/blood.2022015554.
25. Bowley SR, Fang C, Merrill-Skoloff G, Furie BC, Furie B. Protein disulfide isomerase secretion following vascular injury initiates a regulatory pathway for thrombus formation. Nat Commun. 2017;8:14151. https://doi.org/10.1038/ncomms14151.

26. Lv K, Chen S, Xu X, Chiu J, Wang HJ, Han Y, et al. Protein disulfide isomerase cleaves allosteric disulfides in histidine-rich glycoprotein to regulate thrombosis. Nat Commun. 2024;15:3129. https://doi.org/10.1038/s41467-024-47493-0.
27. von Brühl ML, Stark K, Steinhart A, Chandraratne S, Konrad I, Lorenz M, et al. Monocytes, neutrophils, and platelets cooperate to initiate and propagate venous thrombosis in mice in vivo. J Exp Med. 2012;209:819–35. https://doi.org/10.1084/jem.20112322.
28. Essex DW, Li M. Redox control of platelet aggregation. Biochemistry. 2003;42:129–36. https://doi.org/10.1021/bi0205045.
29. Skarnes WC, Rosen B, West AP, Koutsourakis M, Bushell W, Iyer V, et al. A conditional knockout resource for the genome-wide study of mouse gene function. Nature. 2011;474:337–42. https://doi.org/10.1038/nature10163.
30. Viviano J, Brecker M, Ferrara-Cook C, Suaud L, Rubenstein RC. ERp29 as a regulator of insulin biosynthesis. PLoS ONE. 2020;15:e0233502. https://doi.org/10.1371/journal.pone.0233502.
31. Baryshev M, Sargsyan E, Mkrtchian S. ERp29 is an essential Endoplasmic reticulum factor regulating secretion of thyroglobulin. Biochem Biophys Res Commun. 2006;340:617–24. https://doi.org/10.1016/j.bbrc.2005.12.052.
32. Das S, Smith TD, Sarma JD, Ritzenthaler JD, Maza J, Kaplan BE, et al. ERp29 restricts Connexin43 oligomerization in the Endoplasmic reticulum. Mol Biol Cell. 2009;20:2593–604. https://doi.org/10.1091/mbc.e08-07-0790.
33. Cormet-Boyaka E, Jablonsky M, Naren AP, Jackson PL, Muccio DD, Kirk KL. Rescuing cystic fibrosis transmembrane conductance regulator (CFTR)-processing mutants by transcomplementation. Proc Natl Acad Sci U S A. 2004;101:8221–6. https://doi.org/10.1073/pnas.0400459101.
34. Grumbach Y, Bikard Y, Suaud L, Chanoux RA, Rubenstein RC. ERp29 regulates epithelial sodium channel functional expression by promoting channel cleavage. Am J Physiol Cell Physiol. 2014;307:C701–9. https://doi.org/10.1152/ajpcell.00134.2014.
35. Yan B, Smith JW. A redox site involved in integrin activation. J Biol Chem. 2000;275:39964–72. https://doi.org/10.1074/jbc.M007041200.
36. Passam F, Chiu J, Ju L, Pijning A, Jahan Z, Mor-Cohen R, et al. Mechano-redox control of integrin de-adhesion. Elife. 2018;7. https://doi.org/10.7554/eLife.34843.


## Publisher's note